Matthew S. Munson
J. Mark Meacham
David Ross
Laurie E. Locascio

Biochemical Science Division, National Institute of Standards and Technology, Gaithersburg, MD, USA

Received March 31, 2008
Revised May 20, 2008
Accepted May 20, 2008

Research Article

Development of aptamer-based affinity assays using temperature gradient focusing: Minimization of the limit of detection

A method is described for an aptamer-based affinity assay using a combination of two nonconventional techniques, temperature gradient focusing (TGF) and field-amplified continuous sample injection TGF (FACSI-TGF), with fluorescence detection. Human immunodeficiency virus reverse transcriptase (HIVRT) is used as the protein target for the assay. The TGF and FACSI-TGF assays are compared to similar results obtained with conventional CE. A range of starting aptamer concentrations are used to determine the optimal LOD for human immunodeficiency virus reverse transcriptase (HIVRT) using each approach. The results indicate that the LODs for HIVRT obtained with TGF and FACSI-TGF are comparable to or even lower than the LODs obtained with conventional CE in spite of the inferior detector used for the TGF and FACSI-TGF assays (arc lamp and low-cost CCD for TGF *versus* LIF with PMT for CE). It is hypothesized that this is due to the greater reproducibility of the TGF and FACSI-TGF techniques since they do not employ a defined sample injection. The lowest LOD achieved with the new aptamer assay approach is more than an order of magnitude lower than that reported for a similar CE-based aptamer assay for the same target.

Keywords:
Aptamer / Capillary electrophoresis / Human immunodeficiency virus reverse transcriptase / Temperature gradient focusing DOI 10.1002/elps.200800210

1 Introduction

Aptamers are short single strands of DNA or RNA that interact specifically with a target molecule [1, 2]. Aptamers are attractive alternatives for antibodies because they are simpler to label fluorescently, easier to produce as they require no host animal, and have more predictable electrophoretic behavior. These molecules are being considered by many groups as functional replacements for antibodies as affinity recognition molecules; however, there is still significant research to be done to assess their broad applicability [3]. There have been many different approaches taken for the development of analytical platforms using aptamers as in the following review articles [4–6]. One established analytical use of aptamers is as probe molecules in affinity probe CE (APCE). For example, German *et al.* [7] were the first to demonstrate the use of fluorescently labeled DNA aptamers for noncompetitive APCE for thrombin and human IgE. APCE has also been used with aptamers for the detection of ricin [8], neuropeptide Y [9], protein farnesyltransferase [10], and HIV reverse transcriptase (HIVRT) [11, 12].

APCE has been used successfully for the development of affinity assays [13–16], as a technique for the determination of interaction strengths between biomolecules [17, 18], and as a technique for the purification of affinity reagents for a specific target [10, 12, 19–21]. One of the most commonly encountered obstacles in APCE is the nonspecific adsorption of sample matrix components to separation channel surfaces. This can lead to degradation of system performance and is particularly significant in microfluidic devices due to the associated increase in the surface area to volume ratio. Electrokinetic separations are sensitive to nonspecific adsorption because they rely on EOF, which is dependent on the ζ potential of the channel walls. Great effort has been expended in the characterization and mitigation of this problem utilizing static or dynamic surface coatings to pre-

Correspondence: Dr. Matthew S. Munson, NIST, 100 Bureau Drive, MS 8313, Gaithersburg, MD 20899-8313, USA
E-mail: matt.munson@nist.gov
Fax: +1-301-975-4845

Abbreviations: APCE, affinity probe CE; **FACSI,** field-amplified continuous sample injection TGF; **HIVRT,** human immunodeficiency virus reverse transcriptase; **TB,** Tris-borate buffer; **TGF,** temperature gradient focusing

vent nonspecific adsorption and provide a reproducible EOF [22–26]. Previously, we have shown that this problem can be avoided by excluding potentially adsorbing molecules from the critical channel segments by exploiting counterflow electrophoresis [27].

Another significant disadvantage of many CE approaches is that the separation can distort the equilibrium distribution of the sample. Many applications specifically take advantage of the shift from equilibrium as the free and bound fractions are separated. However, these methods are typically only applicable to systems with a binding constant in a limited range. One newly described approach is to perform separations on a faster time scale than the binding kinetics [28–30]. However, this approach may not always be feasible for low to moderate affinity interactions, where binding kinetics can be extremely fast. Another approach developed by Krylov and co-workers [10, 31–36] exploits the dissociation of the sample during CE to determine the kinetics of a molecular binding interaction. This technique quantifies the probe, target, and complex species and performs nonlinear regression of the resulting electropherogram to determine the kinetic parameters. Kinetic CE provides more information than the technique described in this report; however, kinetic CE requires injection of all components into the separation channel, subjecting it to problems associated with sample adsorption to the channel walls. These problems are avoided in our work due to counterflow rejection.

In this paper, we demonstrate the use of a counterflow separation technique, temperature gradient focusing (TGF) [27, 37–40] and field-amplified continuous sample injection-TGF (FACSI-TGF) [41], for the determination of protein concentrations using aptamers as affinity probes. We use HIV reverse transcriptase (HIVRT) as the protein target, and an aptamer sequence for HIVRT published by Mosing *et al.* [12]. In addition, we explore the experimental parameters that lead to minimization of the LOD of the assay, and demonstrate that the technique can also be used to measure the interaction strength between the affinity molecule and the target.

Our previous efforts had been focused on the detection of small molecules (or characterization of their affinities) using proteins as affinity molecules. Both direct affinity assay of observable (fluorescent) analytes and competitive determination of concentration and affinity were demonstrated [27]. The primary limitations of this technique are that it requires either a fluorescent target molecule or a fluorescent analog of the target that competes for the same binding site on the affinity molecule. In addition, due to problems with nonspecific adsorption, it is beneficial if the observed species, whether it is the target or the analog, has a higher electrophoretic mobility than the affinity molecule. In this work, we show that these limitations are effectively overcome by using a fluorescently labeled DNA aptamer as the affinity molecule, thereby greatly expanding the class of analytes that can be detected. Custom DNA sequences are readily available from commercial vendors and can be ordered with single-fluorophore end-labels. In addition, the electrophoretic mobility of the aptamers is greater than most proteins, so that counterflow rejection can be used to avoid nonspecific adsorption.

2 Materials and methods

2.1 Disclaimer

Certain commercial equipment, instruments, or materials are identified in this report to specify adequately the experimental procedure. Such identification does not imply recommendation or endorsement by the National Institute of Standards and Technology nor does it imply that the materials or equipment identified are necessarily the best available for the purpose.

2.2 Chemicals and reagents

Fused-silica capillary (30 μm or 75 μm id; 360 μm od) was obtained from Polymicro Technologies, LLC (Phoenix, AZ). Polycarbonate sheets were from McMaster-Carr (Atlanta, GA). BSA (Fraction V, essentially fatty acid free >96%) (BSA) was obtained from Sigma–Aldrich (St. Louis, MO). All solutions were made from ≥18 MΩ·cm deionized water (Easypure II, Barnstead Internation, Dubuque, IA). ssDNA with the sequence 5′-AGC AGC ACA GAG GTC AGA TGG CAG GTT TCG ACG TAC AAT GCT ATG GAG GCT TTA TGA TCG CCT ATG CGT GCT ACC GTG AA-3′(clone 4.3 from Mosing *et al.* [12]) was purchased from Oligos *etc.* (Wilsonville, OR) labeled at the 5′-end with 6-carboxyfluorescein (FAM). Recombinant HIV reverse transcriptase (HIVRT) was purchased from Worthington Biochemical Corporation (Lakewood, NJ). Tris was purchased from Amresco (Solon, OH). All other chemicals were obtained from Sigma–Aldrich and were of the highest purity available. All TGF experiments utilized a run buffer consisting of 0.5 mol/L Tris and 0.5 mol/L boric acid (TB). This buffer shows a decrease in ionic strength with increasing temperature and was selected on the basis of its suitability for TGF as evaluated previously. A guide for the selection of TGF buffers at various pH levels has been published elsewhere [38]. Working stock solutions of aptamer were prepared at a concentration of 100 nmol/L in TB with 5 mg/mL BSA. Working stock solutions of HIVRT were prepared at 1 μmol/L with 5 mg/mL BSA and at 250 nmol/L with 5 mg/mL BSA.

2.3 TGF instrumentation

Experiments were performed on an apparatus previously described for use in scanning TGF [40]. Briefly, an optical window approximately 7 mm wide was burned into a 3 cm long capillary prior to enclosure between two polycarbonate sheets; the sandwich assembly was then placed in a hydraulic press at 500 kg, heated to 200°C, and cooled to 120°C prior to releasing pressure. This process ensured good mechanical

stability of the separation channel and thermal contact to the exposed silica region and the temperature controlled anchor blocks. The separation channel was fixed in a holder consisting of two thermally regulated copper blocks. One capillary end was inserted into a 360 μm diameter hole drilled into a Delrin™ sample reservoir containing 125 μL of sample held at −3 kV while the other end was inserted through a Teflon backed silicone septum into a grounded polysulfone run buffer reservoir containing 1500 μL of buffer connected to a precision pressure controller (Series 600, Mensor, San Marcos, TX) with a range of ±13.8 kPa. Unless otherwise noted, the sample was anchored to a copper block regulated at a temperature of 20°C (cold edge). A section of the middle of the capillary (about 10 mm from the input end and 6 mm long) was anchored to a second copper block maintained at an elevated temperature (hot edge). The capillary was conditioned with 1 mol/L sodium hydroxide for 15 min followed by deionized water and run buffer prior to the first use and thoroughly flushed with run buffer between analyses.

Experiments were performed on a Axioskop 2 plus fluorescent microscope (Carl Zeiss, Thornwood, NY) equipped with a long-working distance 5 × objective (numerical aperture, NA = 0.13), 100 W Hg arc lamp, 12-bit color CCD camera (CFW-1312C, Scion Corporation, Frederick, MD), and appropriate fluorescence filter sets (excitation: band pass 450–490 nm, emission: long pass 515 nm). All instrument control and data acquisition were performed using a LabVIEW-based software platform (National Instruments, Austin, TX) written in-house. The detection spot (75 μm long × 30 μm wide) was located 300 μm from the hot edge of the temperature gradient. The camera exposure time was 1.0 s at a gain of 5 dB. Figure 1 shows a schematic and photograph of the TGF apparatus.

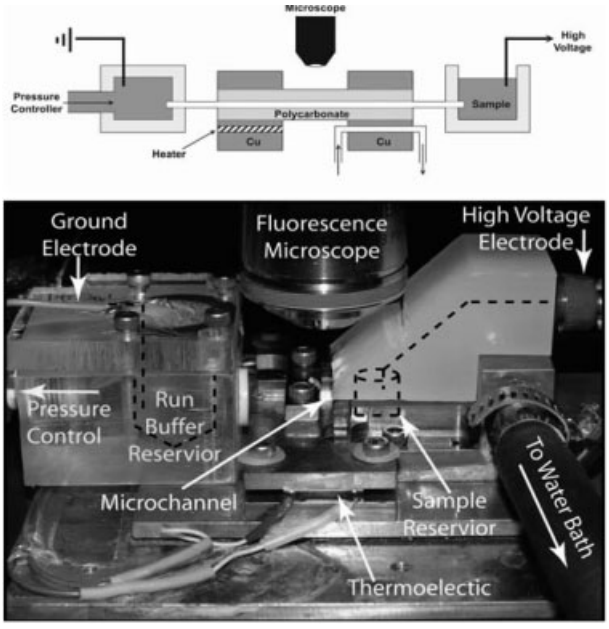

Figure 1. Schematic and photograph of TGF apparatus showing key components.

2.4 TGF separation conditions

A voltage of −3 kV (Stanford Research Systems, Sunnyvale, CA) was applied at the sample reservoir (run buffer reservoir grounded) giving an approximate field strength of −1 kV/cm. For LOD experiments, a temperature gradient of 22.5°C/mm (65–20°C) was applied across a 2 mm segment of the 30 mm long capillary. Complete calibration curves were collected and dissociation constant (K_d) determinations were made using temperature gradients of 30°C/mm (80–20°C), 22.5°C/mm (65–20°C), and 15°C/mm (50–20°C). The applied pressure used to control the counterflow was initially held at +100 Pa for 30 s under the applied voltage. The pressure was then gradually reduced in −2 Pa increments with a 2 s hold time at each pressure to −900 Pa. The average current obtained in these experiments was 24 μA over the course of the 7.5 min experiment. Given the volume of our sample reservoir (125 μL), this corresponds to a 0.87 mmol/L increase in concentration of OH^- ions in the sample, which is negligible in comparison to the 500 mmol/L buffer strength. Experiments exploring the full dynamic range of the assay scheme employed a nominal aptamer concentration of 10 nmol/L and 1 mg/mL BSA. The HIVRT concentration was varied from 0 to 50 nmol/L. Experiments designed to minimize the LOD utilized an aptamer concentration from 0.25 to 10 nmol/L, 1 mg/mL BSA, and three or four HIVRT concentrations (including 0 nmol/L) covering the linear part of the response curve. TGF experiments used samples with buffer concentrations equal to the concentration in the separation buffer (0.5 mol/L TB) while FACSI-TGF samples had a buffer concentration of 0.1 mol/L TB. Samples were incubated for 10 min at 20°C prior to the beginning of each measurement. Representative electropherograms for TGF and FACSI-TGF are shown in Figs. 2a and b, respectively.

2.5 CE experimental conditions

CE was performed on a Beckman Pace MDQ CE system (Beckman Coulter, Fullerton, CA). LIF detection was used with an excitation wavelength of 488 nm and an emission bandpass filter of 520 nm. A 75 μm id, 50 cm effective length (60 cm total length) bare fused-silica capillary (Beckman Coulter, Fullerton, CA) was used and thermostated at 20°C. Separations were carried out in the buffer reported by Mosing *et al.* [12] for the CE SELEX of the aptamer sequence (25 mmol/L Tris, 192 mmol/L glycine, 5 mmol/L KH_2PO_4, pH 8.3). The voltage applied during separation was 30 kV (normal polarity). Injections were made at 3447 Pa (0.5 psi) for 3 s duration. The capillary was rinsed for 10 min with 1 mol/L NaOH for 5 min with deionized water and for 1 min with run buffer prior to each separation.

Experiments designed to minimize the LOD utilized an aptamer concentration from 0.25 to 10 nmol/L, 1 mg/mL BSA, and three or four HIVRT concentrations (including 0 nmol/L) covering the linear part of the response curve.

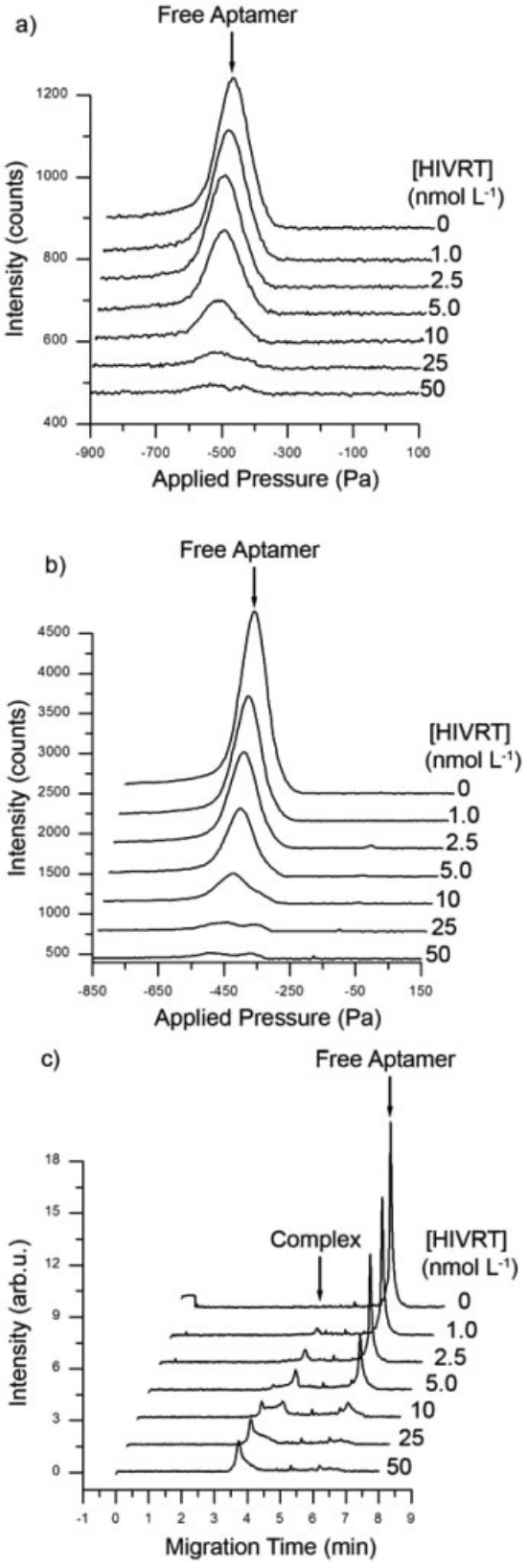

Figure 2. Representative electropherograms for (a) TGF, (b) FACSI-TGF, and (c) CE analysis aptamer/protein binding.

After mixing, each sample was incubated for 10 min at 20°C prior to the injection. For an LOD determination, each measurement was repeated three times on the same day with the same batch of aptamer and HIVRT.

For experiments exploring the full dynamic range of the assay, each sample contained a nominal aptamer concentration of 10 nmol/L, 1 mg/mL BSA, and an HIVRT concentration from 0 to 50 nmol/L. After mixing, each sample was incubated for 10 min at 20°C prior to the injection. Each measurement was repeated three times with one batch of aptamer and HIVRT, and then 2 weeks later repeated an additional four times with a second batch of aptamer and HIVRT (from the same lot). The two datasets were consistent, though there was slightly less variation of the peak height and area within the second set of measurements, so those data were used for the detailed analyses presented below. Representative electropherograms for each HIVRT concentration are shown in Fig. 2c.

2.6 Data analysis

For TGF, all data points were collected in triplicate and error bars reported are the SD of the mean, unless otherwise noted. Concentration of unbound aptamer was assumed to be directly proportional to the focused peak height as demonstrated in previous work [27, 40, 41]. Dissociation constants, other fitting parameters, and the related uncertainties were determined using nonlinear least squares regression analysis performed using Mathematica (Wolfram Research, Champaign, IL).

For CE, peak heights were calculated using the 32 Karat software (Beckman Coulter, Fullerton, CA). Corrected peak areas (area divided by migration time) for both the free aptamer and the aptamer/HIVRT complex were calculated using Mathematica (Wolfram Research, Champaign, IL). The aptamer/HIVRT complex produced two peaks in the electropherograms. Consequently, the peak area of both peaks (and the region between them) was used as the peak area of the complex.

3 Results and discussion

TGF is an electrokinetic separation technique that relies on a buffer exhibiting a temperature dependent ionic strength. Briefly, TGF balances the electrophoretic flux of ionic analytes with the convective flux of the run buffer through a separation channel under an imposed temperature gradient. The run buffer is chosen so that the ionic strength, and therefore electrophoretic velocity, varies with temperature. The convective velocity can be adjusted so that the net flux of each analyte (the sum of the electrophoretic and convective fluxes) is zero at a unique point in the channel. This leads to simultaneous separation and concentration of analytes based on their electrophoretic mobilities [39]. For quantitative measurements with TGF, a "scanning" approach is used

during which the convective velocity is varied over time so that each analyte species is sequentially focused, mobilized past a fixed detection point, and eluted to waste [40]. For a fixed set of experimental parameters, the resulting peak height has been demonstrated to be a linear function of the species concentration in the sample reservoir, making the development of equilibrium binding assays fairly straightforward [27, 40, 41]. The counterflow also allows for the sampling of mixtures without disturbing the equilibrium distribution [27].

For the TGF assay described here, the only species measured was the free aptamer, the species of highest mobility. The free aptamer peak height as a function of the concentration of HIVRT can be seen in Fig. 3. The form of the binding curve can be calculated using mass balance relationships and the mathematical definition of K_d:

$$A = A_o - \frac{1}{2}\left(A_o + T_o + K_d - \sqrt{(A_o + T_o + K_d)^2 - 4A_oT_o}\right) \quad (1)$$

where A is the concentration of free aptamer, A_o is the initial concentration of aptamer, and T_o is the initial concentration of target molecule. Aptamer concentrations (A, A_o) are related to measured intensities using a one-point calibration curve in the absence of protein target. Nonlinear regression of the data to Eq. (1) using K_d and A_o as fitting parameters was performed giving a K_d value of 1.65 ± 0.23 and 6.67 ± 0.58 nmol/L for A_o (best fit curve shown in Fig. 3). The listed uncertainties are the asymptotic standard errors computed by the regression algorithm. The K_d value obtained is over an order of magnitude greater than the value reported by Mosing *et al.* [12] (190 pmol/L). We speculate that the fluorescent label used is partially responsible for the decrease in affinity (increase in K_d). In addition, our experiments were conducted using a different buffer system and in the presence of BSA, which was absent in the work of Mosing *et al.* [12]. In the absence of BSA added to the stock solutions we observed significant decrease in apparent HIVRT concentration with sample age over the course of a single day, most likely a result of denaturation of the HIVRT or nonspecific adsorption of HIVRT to the walls of the sample vials.

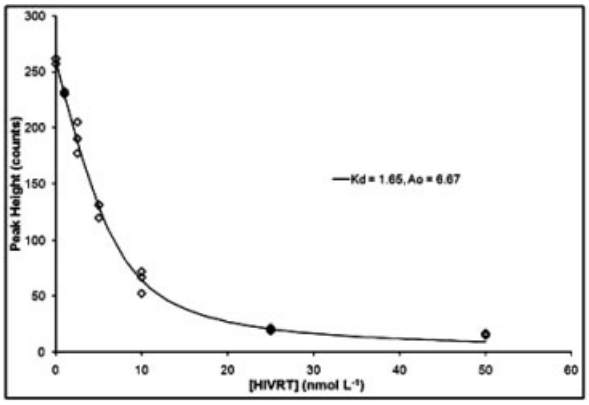

Figure 3. TGF binding curve for a 50–20°C temperature gradient. Free aptamer peak height is shown as a function of target concentration. Points from replicate measurements ($n = 3$) are shown in place of error bars. Error bars on each single data point are vanishingly small in comparison to the variation from repeated measurements, and are therefore omitted. Solid curve: nonlinear regression of the data using Eq. (1), giving K_d = 1.65 nmol/L.

In addition, the determined value for A_o did not match the expected value of 10 nmol/L. Possible reasons for this are hydrolysis of the bond between the aptamer and label, incomplete labeling of the aptamer sequence, nonspecific adsorption of the aptamer to the walls of the stock solution container/sample vials, binding of the aptamer or its label (FAM) to the BSA in solution, or the binding between aptamer and target not being 1:1.

The data set shown in Fig. 2 was collected using a temperature gradient of 15°C/mm (50–20°C). The temperature gradient in a TGF experiment is one parameter that affects the extent of focusing, which in turn impacts the magnitude of the signal observed. Peak height as a function of target concentration was measured at three temperature gradients 30, 22.5, and 15 C/mm. The resulting binding curves can be seen in raw intensity and normalized to the peak height obtained when [HIVRT] = 0 nmol/L formats in Figs. 4a and b, respectively. The K_d determined from the 30 and 22.5°C/mm temperature gradients are statistically consistent with the value determined above for the 15°C/mm temperature gradient. As a result, the binding curves collapse on each other when normalized. From this we conclude that the two ends of the channel are sufficiently thermally isolated from each other that the temperature on the hot side of the channel does not impact the incubation temperature of the sample. In addition, this supports our claim that aptamer/target complex was excluded from the channel. If the complex had entered the channel, we anticipate the different temperatures on the hot end would have influenced the apparent binding as a result of aptamer–target denaturation.

For comparison, a similar assay was also developed using a commercial CE system. The same buffer system used by Mosing *et al.* [12] for the selection of the aptamer was used here for the CE-based assay (25 mmol/L Tris, 192 mmol/L glycine, 5 mmol/L KH_2PO_4, pH 8.3). A plot of the corrected area of the free aptamer peak *versus* HIVRT concentration for the CE assay can be seen in Fig. 5. Nonlinear regression to Eq. (1) using K_d and A_o as fitting parameters was performed giving a K_d value of (600 ± 150) pmol/L and (5.1 ± 0.5) nmol/L for A_o. The listed uncertainties are the asymptotic standard errors computed by the regression algorithm. In this case, the computed value of K_d is approximately a factor of three larger than the value reported for this sequence/target by Mosing *et al.* [12], indicating that the most likely cause of the difference is either the fluorescent label or the use of BSA in our assay.

For determination of the LOD for the HIVRT assays, the most significant portion of the binding curve is the behavior

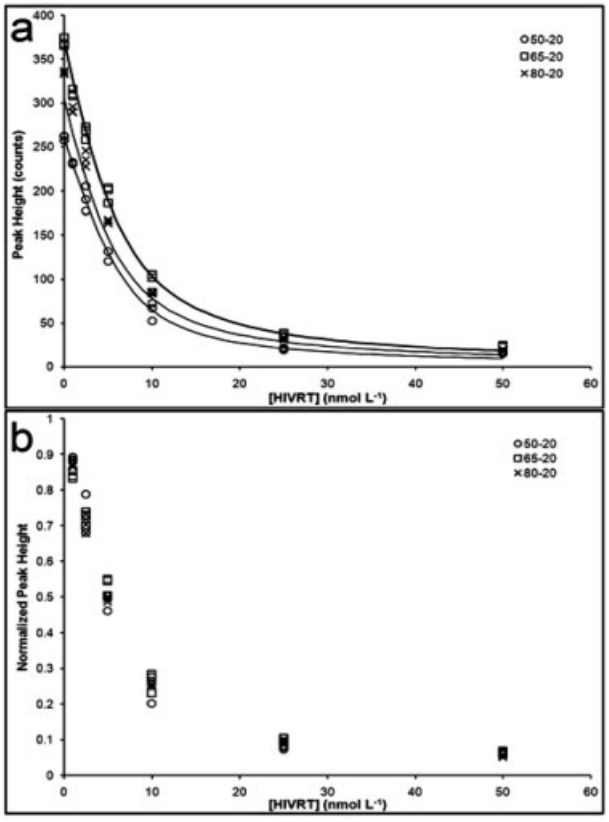

Figure 4. (a) Raw TGF binding curve for 50–20°C (○), 65–20°C (□), and 80–20°C (x) temperature gradients. Free aptamer peak height is shown as a function of target concentration. Points from replicate measurements (n = 3) are shown in place of error bars. Error bars on each single data point are vanishingly small in comparison to the variation from repeated measurements, and are therefore omitted. Solid curve: nonlinear regression of the data using Eq. (1). The fit K_d's and their confidence intervals are overlapping for all three data sets. (b) Normalizing the raw curves using the [HIVRT] = 0 nmol/L data point from each set causes the datasets to become superimposed demonstrating that the hot side temperature only has an impact on the degree of focusing, not on the binding reaction in the sample.

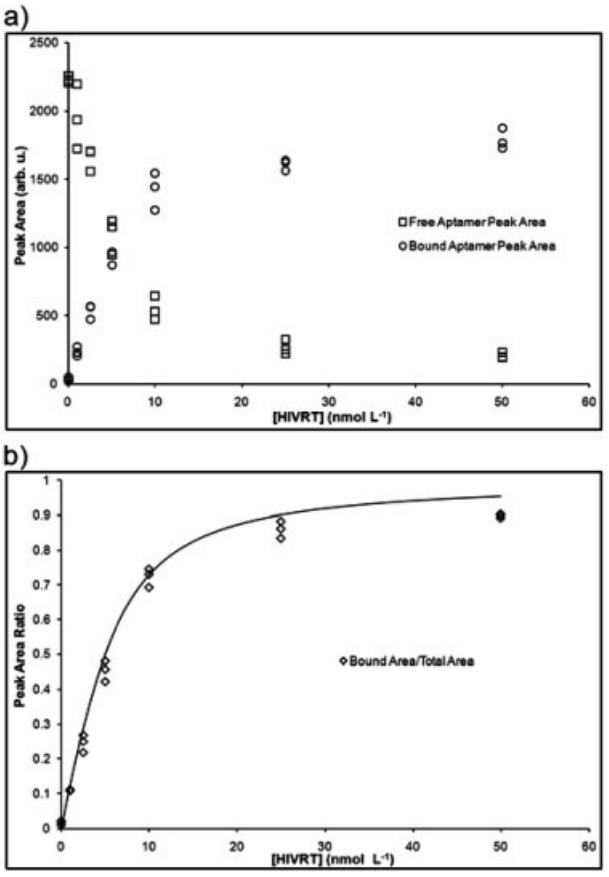

Figure 5. CE binding curves. (a) Free aptamer (□) and aptamer/ligand complex (◇) peak areas are shown. (b) Data are reduced to the peak area ratio (complex area divided by total area). Nonlinear regression yields a K_d of 600 pmol/L. Points from replicate measurements (n = 4) are shown in place of error bars. Error bars on each single data point are vanishingly small in comparison to the variation from repeated measurements, and are therefore omitted.

as the input HIVRT concentration approaches zero. Computing a Maclaurin series expansion of Eq. (1), the binding curve can be approximated as a linear expression:

$$A = A_o - \frac{A_o T_o}{A_o + K_d} \quad (2)$$

Assuming that the measured signal (peak height or area) is proportional to A, the LOD is the value of T_o at which A differs from A_o by three times the measurement uncertainty (standard error):

$$\mathrm{LOD} = \frac{3\sigma(A_o + K_d)}{A_o} \quad (3)$$

where σ is the standard error of the measurement of the free aptamer concentration, A.

Equation (3) was used for the determination of the LOD of the assay under various experimental conditions. The linear portion of the data was first fit to Eq. (2), and the LOD was calculated with Eq. (3) assuming that the standard error, σ was equal to the SD of the fit residuals. For the TGF assay using the same assay parameters as shown in Fig. 2 (T_o = 10 nmol/L, 15°C/mm temperature gradient), the LOD was 520 pmol/L. In comparison, the LOD of the CE-based assay, using the free aptamer peak height (or area) as the signal, was 970 pmol/L (1.3 nmol/L). That the LOD with the CE-based assay was higher than that of the TGF-based assay was somewhat surprising given that the detection system for the CE-based assay (a commercial LIF/PMT system) should be intrinsically much better than that used for the TGF-based assay (fluorescence microscope with mercury arc lamp and low-cost, uncooled CCD camera). This indicates that for this relatively high initial aptamer concentration (A_o), the primary factor in determining the LOD is not the ability of the

detector to accurately measure a fluorescence signal, but the ability of the technique to reproducibly deliver the same amount of sample to the detector for measurement, and in this respect the TGF technique – with a continuous rather than defined injection – appears to be slightly better.

One of the advantages of the CE-based assay, however, is that it provides a measurement of both the free aptamer as well as the aptamer/HIVRT complex. Using the peak area of the complex, the CE assay gives an LOD of 650 pmol/L, whereas using the ratio of the complex peak area to the total (free plus complex) peak area gives an LOD of 420 pmol/L. The height of the complex peak was not a reliable indicator of HIVRT concentration since there were actually two peaks due to aptamer/HIVRT complex and significant interconversion between the peaks on the time scale of the CE separation (see Fig. 2c). Therefore, the injection-to-injection variability of the CE-based assay can be overcome by using the peak area ratio, giving an LOD slightly better than the TGF-based assay. Note, however, that it may not always be possible to measure both peaks in an affinity assay. In particular, significant interconversion between the free aptamer and aptamer/target complex during the separation and/or inconveniently-placed matrix interferent peaks would make accurate determination of both peaks difficult.

Ultimately, the LOD for a given assay depends on the ability to determine the change in signal as a result of a small portion of the probe molecule binding to the target. For a noncompetitive assay, this ability is controlled by the measurement error and the bound fraction of the number of probe molecules. The fraction bound is a function of the affinity (K_d) and the initial concentration (A_o) of the aptamer. Minimizing the LOD is achieved by minimizing the measurement error, σ, while maximizing the binding. Clearly, the first step in achieving a low LOD is to choose an aptamer with high affinity (low K_d). However, for a given aptamer, buffer system, and detection hardware, there is little that can be done to control the affinity or the measurement error, leaving only the initial aptamer concentration for optimization. Decreasing initial aptamer concentration should result in decreasing LOD. However, this strategy is only successful to the point that the aptamer is detectable above the background. Thus, it is expected that there should be an optimal value of the initial aptamer concentration, and that the use of focusing or other concentration enhancement techniques should shift the optimal value to lower initial aptamer concentrations to give lower LODs.

To determine the optimal initial aptamer concentration for the TGF assay, the linear portion of the binding curve was measured for different initial aptamer concentrations ranging from 0.25 to 10 nmol/L. The peak height in the absence of HIVRT was measured for each aptamer concentration as well as at least two HIVRT concentrations near the anticipated LOD. Plots of the resulting peak height as a function of HIVRT concentration for TGF with different initial aptamer concentrations are shown in Fig. 6a. To understand how the degree of concentration enhancement improves the optimal LOD, the measurements with different initial aptamer concentrations were repeated using field amplified continuous sample injection TGF (FACSI-TGF) [41]. The resulting peak height *versus* HIVRT concentration plots are shown in Fig. 6b. With FACSI-TGF the sample is simply prepared in a buffer of lower conductivity than the TGF run buffer, and the analyte concentration enhancement occurs in two stages, first at the conductivity interface outside the capillary entrance, and then on the temperature gradient. The total concentration enhancement is then the product of the enhancements of the two stages. Similarly, CE measurements were performed using a range of initial aptamer concentrations to determine the optimal LOD for the assay using that technique. Plots of the resulting peak height as a function of HIVRT concentration for CE with different initial aptamer concentrations are shown in Fig. 6c. These data allow us to calculate the LOD for each assay as a function of the input aptamer concentration (Fig. 6d). For CE, the LOD was calculated using both the free aptamer peak height and the corrected peak area ratios.

For TGF, the optimal aptamer concentration was 5 nmol/L, giving an LOD of 220 pmol/L. For FACSI-TGF, the optimal aptamer concentration and LOD were both lower (2.5 nmol/L and 84 pmol/L) as expected due to the double focusing effect. For CE, using the free peak height, the optimal aptamer concentration and optimal LOD were 0.5 nmol/L and 170 pmol/L; and for CE using the peak area ratio, the optimal aptamer concentration and LOD were 2.5 nmol/L and 280 pmol/L. Again, it was somewhat surprising to find that the best LOD was not given by the technique using the best detector.

Comparing the LOD *versus* aptamer concentration curves provides a valuable tool for the comparison of the different assay techniques. To construct a simple model of the expected form of the LOD *versus* aptamer concentration curves, we assume that the uncertainty associated with the measurement of the peak height or area has a component that is proportional to the magnitude of the signal (α) and a component that is constant (β):

$$\sigma = \alpha S + \beta \tag{4}$$

The proportional component, α, is a measure of the repeatability of the assay as a whole and encompasses systematic factors such as pipetting error and sample injection error. The constant component, β, is a measure of the LOD of the aptamer in the absence of HIVRT.

Using Eqs. (2, 4) we can calculate a simple functional form for the LOD resulting from the measurements of the free aptamer peak height:

$$\mathrm{LOD}_{\mathrm{free}} = \frac{3(A_o + K_d)(\alpha A_o + \beta)}{A_o} \tag{5}$$

Although Eq. (5) is probably too much of an oversimplification to be used quantitatively, it can be used to draw some qualitative conclusions from the data. In the limit

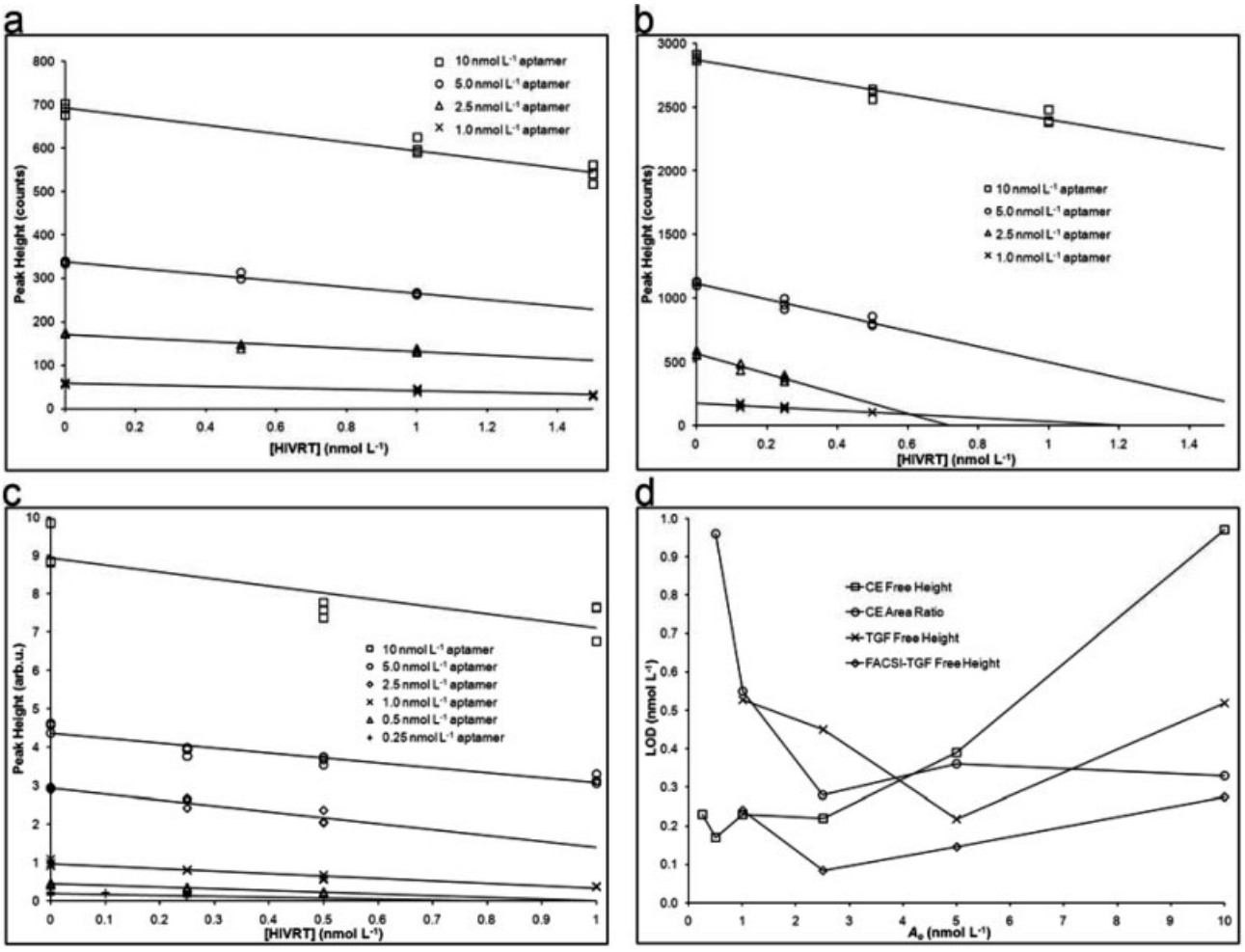

Figure 6. Determination of the LOD as a function of initial aptamer concentration. Low target concentrations are used to map a linear portion of binding curves for (a) TGF, (b) FACSI-TGF, and (c) CE at a range of aptamer concentrations. Linear regression using Eq. (2) allowed determination of the LOD using Eq. (3). (d) The LOD is plotted as a function of initial aptamer concentration for FACSI-TGF (◇), TGF (x), CE based on the free aptamer peak height (□) and CE based on the peak area ratio (○).

of large initial aptamer concentration (A_o), $LOD_{free} \cong 3\alpha A_0$, indicating that the slope of the LOD *versus* A_o curve, at high A_o, is a measure of the repeatability of the technique (independent of the detector used). The data of Fig. 6d would then indicate that the TGF and FACSI-TGF techniques are more repeatable than the CE technique.

We hypothesize that the reason for this is that the CE assay requires an injection of a defined quantity of material into the channel. In the absence of an internal standard, the impact of the fluctuations in injection volume can have a significant impact on the repeatability of the CE assay. In TGF and FACSI-TGF, there is no injection step and thus there is one fewer source of variability in these assays.

Analysis of the CE data using the peak area ratio to determine the target molecule (HIVRT) concentration gives a substantially different behavior. A result similar to Eq. (5) can be calculated (assuming a similar detector response for the bound aptamer and free aptamer and that the bound and free aptamer concentrations sum to A_o):

$$LOD_{ratio} = \frac{3\beta(A_o + K_d)}{A_o} \quad (6)$$

In this case, the LOD_{ratio} is predicted to be a monotonically decreasing function of A_o, and the optimal LOD_{ratio} (at very high A_o) is predicted to be lower than the optimal LOD_{free} (assuming reasonable values of α). However, over the range of A_o used here, the LOD_{ratio} *versus* A_o curve appears to be nonmonotonic (see Fig. 6d), and the lowest LOD_{ratio} achieved (280 pmol/L) was significantly higher than the optimal LODs obtained using any of the techniques for measurement of the free aptamer peak height. This challenges the oft-stated conventional wisdom that lower LODs can be achieved by monitoring the appearance of a small peak above a baseline signal than by monitoring a small

decrease in a large signal. We believe that measurement of the bound peak did not result in improved LODs because of the disassociation of the complex during the separation. If upon binding, there is no impact on the fluorescence and there is no disassociation, conservation of mass would dictate that the change in the free peak would be identical to the change in the bound peak, resulting in lower LODs by using the bound peak for quantification. However, there is significant tailing of the complex peak toward the free aptamer peak, as shown in Fig. 7. This disassociation leads to a smaller signal in the bound peak but has minimal impact on the free peak. The result is that the change in the area of the free peak is larger than the change in size of the bound peak. In theory it should be possible to integrate the entire electropherogram to mitigate the impact of the tailing on analysis, however, the presence of other small interfering peaks between the free and the bound peaks makes this problematic.

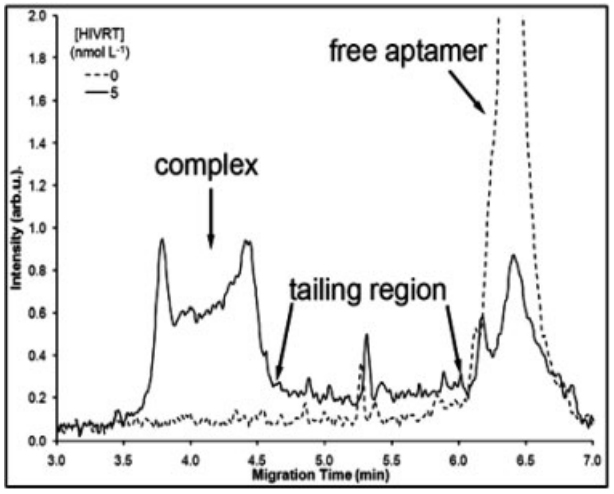

Figure 7. During the course of the CE separation, dissociation of the aptamer/target complex occurs, demonstrated by the elevated baseline between the complex and free aptamer peaks in the electropherogram. This has a significant impact on quantification using the bound peak, but little impact on quantification using the free aptamer peak.

4 Concluding remarks

In this report, we have demonstrated the use of the counterflow electrophoresis technique, TGF, for aptamer-based, noncompetitive protein assays. The combination of fluorescently labeled aptamers with the counterflow separation is particularly powerful as nucleic acids probes are significantly more stable than antibodies, and are typically of greater electrophoretic mobility than proteins due to their high charge density. Using a single aptamer as the affinity molecule we were able to achieve three orders of magnitude dynamic range with an optimized LOD of 84 pmol/L. In comparison, Pavski and Li [11] reported a CE-based HIVRT assay using aptamers with an LOD of approximately 5 nmol/L based on quantitation of the free aptamer peak. Haes *et al.* [8] reported a similar assay for ricin with an LOD of 500 pmol/L based on quantitation of the bound complex peak. This work provides a solid foundation for further development of protein assays, as other aptamers should have very similar electrophoretic behavior. Future steps include the development of multiplexed assays based on using different dye labels for each aptamer and work in difficult sample matrices such as serum.

This work was supported by an NRC postdoctoral fellowship (Meacham). We thank Michael T. Bowser for providing us with the sequence for the HIVRT aptamer before its publication.

The authors have declared no conflict of interest.

5 References

[1] Ellington, A. D., Szostak, J. W., *Nature* 1990, *346*, 818–822.

[2] Tuerk, C., Gold, L., *Science* 1990, *249*, 505–510.

[3] Jayasena, S. D., *Clin. Chem.* 1999, *45*, 1628–1650.

[4] Tombelli, S., Minunni, M., Mascini, M., *Biomol. Eng.* 2007, *24*, 191–200.

[5] Hamula, C. L. A., Guthrie, J. W., Zhang, H. Q., Li, X. F., Le, X. C., *Trends Anal. Chem.* 2006, *25*, 681–691.

[6] Tombelli, S., Minunni, A., Mascini, A., *Biosens. Bioelectron.* 2005, *20*, 2424–2434.

[7] German, I., Buchanan, D. D., Kennedy, R. T., *Anal. Chem.* 1998, *70*, 4540–4545.

[8] Haes, A. J., Giordano, B. C., Collins, G. E., *Anal. Chem.* 2006, *78*, 3758–3764.

[9] Mendonsa, S. D., Bowser, M. T., *J. Am. Chem. Soc.* 2005, *127*, 9382–9383.

[10] Berezovski, M., Drabovich, A., Krylova, S. M., Musheev, M. *et al.*, *J. Am. Chem. Soc.* 2005, *127*, 3165–3171.

[11] Pavski, V., Le, X. C., *Anal. Chem.* 2001, *73*, 6070–6076.

[12] Mosing, R. K., Mendonsa, S. D., Bowser, M. T., *Anal. Chem.* 2005, *77*, 6107–6112.

[13] Guzman, N. A., Phillips, T. M., *Anal. Chem.* 2005, *77*, 60A–67A.

[14] Heegaard, N. H. H., *Electrophoresis* 2003, *24*, 3879–3891.

[15] Phillips, T. M., Wellner, E., *J. Chromatogr. A* 2006, *1111*, 106–111.

[16] Schou, C., Heegaard, N. H. H., *Electrophoresis* 2006, *27*, 44–59.

[17] Tanaka, Y., Terabe, S., *J. Chromatogr. B* 2002, *768*, 81–92.

[18] Rundlett, K. L., Armstrong, D. W., *Electrophoresis* 2001, *22*, 1419–1427.

[19] Mallikaratchy, P., Stahelin, R. V., Cao, Z. H., Cho, W. H., Tan, W. H., *Chem. Commun.* 2006, 3229–3231.

[20] Mendonsa, S. D., Bowser, M. T., *Anal. Chem.* 2004, *76*, 5387–5392.

[21] Tang, J. J., Xie, J. W., Shao, N. S., Yan, Y., *Electrophoresis* 2006, *27*, 1303–1311.

[22] Shah, J. J., Geist, J., Locascio, L. E., Gaitan, M. *et al.*, *Electrophoresis* 2006, *27*, 3788–3796.

[23] Pallandre, A., de Lambert, B., Attia, R., Jonas, A. M., Viovy, J. L., *Electrophoresis* 2006, *27*, 584–610.

[24] Liu, J. K., Lee, M. L., *Electrophoresis* 2006, *27*, 3533–3546.

[25] Kim, P., Jeong, H. E., Khademhosseini, A., Suh, K. Y., *Lab Chip* 2006, *6*, 1432–1437.

[26] Dolník, V., *Electrophoresis* 2004, *25*, 3589–3601.

[27] Munson, M. S., Meacham, J. M., Locascio, L. E., Ross, D., *Anal. Chem.* 2007, *80*, 172–178.

[28] Clarke, W., Chowdhuri, A. R., Hage, D. S., *Anal. Chem.* 2001, *73*, 2157–2164.

[29] Clarke, W., Schiel, J. E., Moser, A., Hage, D. S., *Anal. Chem.* 2005, *77*, 1859–1866.

[30] Ohnmacht, C. M., Schiel, J. E., Hage, D. S., *Anal. Chem.* 2006, *78*, 7547–7556.

[31] Petrov, A., Okhonin, V., Berezovski, M., Krylov, S. N., *J. Am. Chem. Soc.* 2005, *127*, 17104–17110.

[32] Okhonin, V., Petrov, A. P., Berezovski, M., Krylov, S. N., *Anal. Chem.* 2006, *78*, 4803–4810.

[33] Okhonin, V., Krylova, S. M., Krylov, S. N., *Anal. Chem.* 2004, *76*, 1507–1512.

[34] Krylov, S. N., *Electrophoresis* 2007, *28*, 69–88.

[35] Krylov, S. N., *J. Biomol. Screen.* 2006, *11*, 115–122.

[36] Berezovski, M., Krylov, S. N., *J. Am. Chem. Soc.* 2002, *124*, 13674–13675.

[37] Shackman, J. G., Munson, M. S., Ross, D., *Anal. Bioanal. Chem.* 2007, *387*, 155–158.

[38] Shackman, J. G., Munson, M. S., Kan, C. W., Ross, D., *Electrophoresis* 2006, *27*, 3420–3427.

[39] Ross, D., Locascio, L. E., *Anal. Chem.* 2002, *74*, 2556–2564.

[40] Hoebel, S. J., Balss, K. M., Jones, B. J., Malliaris, C. D. *et al.*, *Anal. Chem.* 2006, *78*, 7186–7190.

[41] Munson, M. S., Danger, G., Shackman, J. G., Ross, D., *Anal. Chem.* 2007, *79*, 6201–6207.

